

RSC Advances

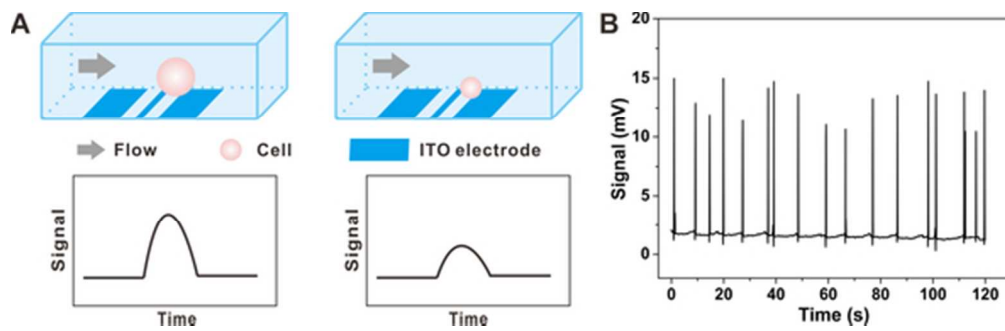


This is an *Accepted Manuscript*, which has been through the Royal Society of Chemistry peer review process and has been accepted for publication.

Accepted Manuscripts are published online shortly after acceptance, before technical editing, formatting and proof reading. Using this free service, authors can make their results available to the community, in citable form, before we publish the edited article. This *Accepted Manuscript* will be replaced by the edited, formatted and paginated article as soon as this is available.

You can find more information about *Accepted Manuscripts* in the [Information for Authors](#).

Please note that technical editing may introduce minor changes to the text and/or graphics, which may alter content. The journal's standard [Terms & Conditions](#) and the [Ethical guidelines](#) still apply. In no event shall the Royal Society of Chemistry be held responsible for any errors or omissions in this *Accepted Manuscript* or any consequences arising from the use of any information it contains.



An integrated and cost-effective microfluidic contactless conductivity cytometer for cell sensing and counting
25x7mm (600 x 600 DPI)

Microfluidic contactless conductivity cytometer for the electrical cell sensing and counting

Duanping Sun, Jing Lu, Zuanguang Chen*

School of Pharmaceutical Sciences, Sun Yat-Sen University, Guangzhou 510006, China

* Corresponding author. Tel.: +86 20 39943044; fax: +86 20 39943071

E-mail address: chenzg@mail.sysu.edu.cn (Zuan-Guang Chen)

Abstract

Microfluidic cytometer has recently attracted increasing attention in cell sensing and counting due to their advantages of high-speed measurement, small sampling size and cost effective. Up to now, conventional microfluidic cytometer usually uses expensive microelectrodes directly in contact with cell suspension to measure the electrical signal changes. In this paper, we introduce a novel approach to perform an integrated microfluidic contactless conductivity cytometer for non-invasive analysis of samples with a small number of cells. The microfluidic chip is composed of a polydimethylsiloxane (PDMS) plate with a narrow microchannel on the top, a 100- μm -thick glass plate in the middle and a glass substrate containing indium tin oxide (ITO) detecting electrodes on the bottom. This contactless measurement approach avoids direct contact between the detection buffer and the ITO electrodes, allowing the electrodes to be easily reused and lowering the cost of the device. When cells flow through a narrow microfluidic channel which is a little larger than the tested cell size, electrical signals are detected by capacitively coupled contactless conductivity detection (C4D) system. Furthermore, human breast cancer (MCF-7) cells and hypertrophic cardiomyocytes (HCM) were used to successfully demonstrate the feasibility of the microfluidic contactless conductivity sensor for counting and detecting cells. Consequently, the designed microfluidic cytometer is cost-effective, easy-to-use and label-free. It is reasonable to expect that this microfluidic cytometer can become a promising tool for the label-free cell counting and point-of-care clinical diagnosis in the developing world.

Keywords: Microfluidic cytometer; Capacitively coupled contactless conductivity detection; Indium tin oxide; Cell sensing; Cell counting

Introduction

It is of great significance that cell counting is a conventional method for diagnosing and monitoring patients in research and medical diagnostic applications. One of the most commonly used methods for cell counting is through the use of flow cytometry¹⁻³. Flow cytometry is a widely used technique in medical diagnostic and biotechnology research due to its fast analysis and high throughput of cells. In conventional flow cytometry, it comprises transporting and counting or examining of cells or particles suspended in a stream of fluid flowing through an optical detection⁴⁻⁶. However, this technology is quite expensive, mechanically complex, and also requires a skilled operator. For example, a commercial optical flow cytometer, Beckman-Coulter FC500, has a very high price tag of about US\$100, 000. The drawbacks limit the use of conventional flow cytometry in many applications, such as for point-of-care diagnostics, as well as limiting the popularity outside of centralized facilities⁷. Thus, it is necessary to develop a less expensive, simpler and easier diagnostic tool which can accurately and rapidly count cells.

In recent years, microfluidic devices have proven to be a leading tool for cell analysis due to their advantages of low cost, high throughput and dimensions comparable to single cell⁸. A number of microfluidic flow cytometers have been designed using conventional materials such as PDMS, silicon and glass and integrated with optical or impedance detections⁹⁻¹¹. In general, optical detection is powerful for counting, characterizing and thus screening cells. For that reason, most microchips based flow cytometers employ an optical detection strategy in which fluorescence

measurements in various manners are representative^{6,10,12}. Although very powerful, the optical microfluidic cytometry often requires complex optical components, including mirror, filter, lens, and so on. To date, the Coulter counter (impedance sensor) is the earliest successful device for measuring impedance changes caused by individual particles or cells of different sizes traversing an orifice. In this system, the passage of a cell through the pore is then detected by a short blockage and decrease of the ionic current through this pore. Impedance cytometry is more preferable because of the lower cost of the readout and detection circuitry as compared to equally sensitive optical methods^{3,13,14}. The existing conventional approaches for microfluidic cytometer usually use planar metal microelectrodes directly in contact with cell suspension to measure the electrical signal or impedance changes¹⁵⁻¹⁷. These methods not only require expensive microelectrodes, but also the fabricated electrodes cannot be reused without a time-consuming cleaning process³. For example, Guo *et al.* present a microfluidic impedance cytometer based on a printed circuit board (PCB) substrate for detection and enumeration of circulating tumor cells. This proposed microfluidic impedance sensor was simply built upon widely available printed circuit board, on which the electrodes had been predeposited for use¹⁸. However, this method cannot avoid direct contact between the detecting buffer and the electrodes, and the electrode substrate cannot be easily recycled.

Conductivity detection is a universal detection technique based on monitoring the conductivity difference through analytic and background solution between two electrodes in the detection zone¹⁹. Capacitively coupled contactless conductivity

detection (C4D) is a particular form of conductivity-based detector, in which the detecting electrodes are not in direct contact with the solution by a thin insulating layer^{20,21}. For the group of electrochemical sensors, C4D is appealing as it can avoid problems commonly found in the contact mode including electrode fouling and bubble formation. The first report about microfluidic system with C4D was published in 2001 by Guijt et al²². Thereafter, with several advances in microfabrication technology, it has resulted in an increasing trend of the development of microchip-based C4D. And the implementation of C4D on microfluidic systems has led to a wide range of applications such as diagnostics, biochemical assays, food safety, homeland security, and many other applications^{23,24}. Despite the large range of successful applications was performed, to our knowledge, there are few papers about microfluidic cytometer based on C4D for cell sensing and counting. More importantly, impedance information as a function of the detection phase angle is not available with the C4D nor is it necessary when aiming only cell counting. Also that the C4D is advantageously simpler than an impedance analyzer because a fixed frequency is set and no phase locked loop detection circuitry is needed. Besides that, indium tin oxide (ITO) electrode has been very popular due to its inexpensive, stable electrochemical and physical properties. The ITO electrode in the study costs less than US\$1.00 and is widely available in the market.

In this paper, we present an integrated and low-cost microfluidic contactless conductivity cytometer for non-damaging cell sensing and counting. This contactless measurement method avoids direct contact between the detection buffer and the ITO

electrodes, allowing the electrodes to be easily reused and lowering the cost of the device. The ITO detecting electrodes are transparent, cost-effective and easily fabricated based on screen-printing technique. Furthermore, the ITO-coated glass makes it possible for mass production of microfluidic cytometers in ordinary laboratories. Compared with the existing microfluidic cytometers, this microfluidic cytometer achieves biocompatible and label-free cell detection without any complex device structures.

Experimental

Materials and reagents

Sylgard 184 silicone elastomer and curing agent were obtained from Dow Corning (Midland, MI, USA). SG2506WC glass (Changsha Shaoguang Chrome Blank Co., Ltd, Changsha, China) was applied as the initial glass wafer for glass mold fabrication. ITO-coated glass (150 nm thick and resistance $< 15 \Omega \text{ square}^{-1}$) was purchased from HIVAC Technology Co., Ltd (Shenzhen, China). Dulbecco's modified Eagle medium (DMEM), fetal bovine serum (FBS), penicillin and streptomycin were from Gibco (Gibco Invitrogen Corp, MD, USA). Phosphate buffered saline (PBS, pH 7.4, 10 mM) was used as detection medium. All solutions were prepared with water by a Millipore Simplicity system (Millipore, Bedford, MA, USA).

Apparatus and softwares

A PDC-32G plasma generator from Harrick Plasma (Harrick Plasma, USA) was applied to bond PDMS and glass chips. A syringe pump (Model TS-1A, Longer pump Corporation, Baoding, China) was applied for cell loading. The C4D is a home-made

instrument that is applied for detecting cells²⁵. The detector was connected to a computer with a chromatography data acquisition unit (ZB-2030, Zhiben analysis technology Corporation, Sichuan, China). Comsol Multiphysics 4.3a (COMSOL AB, Sweden) was used to simulate the fluid flow in the designed microchannel.

Microfluidic device design and fabrication

The experimental setup for integrated microfluidic contactless conductivity cytometer was shown in Fig. 1. The system utilized a syringe pump for cell seeding and a novel microfluidic chip with C4D for counting cells, combined with a data acquisition system and a computer.

Figure 1

The microfluidic chip (as shown in Fig. 2A) was composed of a PDMS plate with a narrow microchannel on the top, a 100- μm -thick glass plate on the middle as the insulating layer and ITO detection electrodes on the bottom glass substrate. The microchip is integrated by using the ITO-coated glass as the substrate of detecting electrodes. Liquid channels were patterned on the top layer of PDMS, which were 20 μm for width, 20 μm for depth and 3 mm in length. Meanwhile, the PDMS chip had the transit region (70- μm -wide, 60- μm -high and 10-mm-long) for cell seeding and the diameter of reservoirs is 2 mm. The bottom ITO-coated glass substrate had three ITO electrodes which were connected to the C4D. Both electrodes (left and right) were 2 mm in width of detection channel and the distance between them was 1 mm. In the middle of two electrodes was a 0.2 mm wide electrode which was connected to ground to decrease noise levels²⁵.

The ITO electrodes were fabricated by screen-printing and chemical etching methods using an ITO-coated glass. The procedures can be referred to the previous study²⁶. Firstly, the ITO-coated glass was sliced into the designed pieces (55 mm × 40 mm). Prior to use, these pieces were cleaned with a chemical detergent solution, distilled water and ethanol for 10 min, respectively. The detecting electrode pattern was designed and then fabricated on a silk-screen. For screen-printing, the oil ink was transmitted through the silk-screen onto the ITO layer by brushing. Once the three electrodes were completed and dried at 80 °C for 15 min, the oil ink was washed away the ITO layer and a wet chemical etching procedure was carried out with mixed solutions (HCL: FeCl₃: H₂O = 1:3:1) for 30 min. After removing the unprotected ITO layer, the desired ITO detecting electrodes were developed on the glass plate (Fig.2B).

The glass mold for PDMS chips was fabricated by glass microlithography. Briefly, we controlled the etching time to make the different depth and width of microchannels in the glass^{27,28}. The designed glass mold was fabricated and then rinsed with pure water and ethanol, dried and stored for PDMS molding. Then, a PDMS chip was cured in an oven for 1 h at 80 °C with the mixing ratio of 10:1 for PDMS base and curing agent. The PDMS replica was peeled off carefully from the glass mold with reservoirs punched and cut into the designed shape. Finally, the top PDMS layer and the middle 100- μ m-thick glass plate were irreversibly bonded by air plasma treatment for 90 s, while the fabricated PDMS/glass chip and the ITO-coated glass substrate were reversibly bonded by simply putting them together (Fig. 2C).

Figure 2

Cell culture and sample preparation

The human breast cancer cell line (MCF-7) was from Cell Bank of Shanghai Institute of Biochemistry and Cell Biology (Shanghai, China). Hypertrophic cardiomyocytes (HCM) of rats were kindly provided by Jing Lu from Sun Yat-Sen University (Guangzhou, China). Isoprenaline (ISO) was used to induce neonatal rat cardiomyocytes to HCM. The size of HCM (a diameter of about 15 μm) is much larger than the MCF-7 cell (a diameter of about 9 μm). MCF-7 is a cell line that was isolated from the human breast tissue and it is a commonly used cell line in cancer research. We used MCF-7 cells as a model to demonstrate the capability of the proposed microfluidic cytometer for detecting cells.

MCF-7 cells and HCM were cultured in the DMEM medium supplemented with 10 % v/v FBS and 1 % v/v penicillin/streptomycin, maintained in a 5 % CO_2 , 95 % humidified atmosphere at 37 °C. Before injection to the microfluidic chip, the cells were re-suspended in the detection solution and diluted to an optimized, relatively low concentration with a density of about 3×10^4 cell mL^{-1} . Prior to experiment, the chip was flushed with 20 mg mL^{-1} BSA solution for 10 min to eliminate non-specific cell adhesion to the surface of the channel. After being washed, detection solution was introduced into the channel to remove all the BSA solution and bubbles.

Cell loading and measurements

Cell suspension was loaded into a microliter syringe and driven through the microchannel in the microfluidic chip using a syringe pump. The pump was used to control the flow rate to make them move one by one into the detection area. The C4D

was connected to a computer with a data acquisition unit and provided three waveforms (sine, square, and triangle) with an oscillation frequency of 0-200 kHz and oscillation voltage of 0-100 V (in Vpp). When a single cell flowed through the narrow detection area, electrical signal was detected by C4D. Between two cell samples, the microchannel was flushed with detection solution to wash away any remaining cells from the previous experiment. In the experiment, we used a C4D and a personal computer to monitor the variation in the output signal as a result of cells flowing through the detecting electrodes.

Results and discussion

System design and simulations

Previous studies have demonstrated that microfluidic impedance cytometry is usually performed as an effective platform in cell sensing and counting^{11,17,29,30}. Most of the existing approaches for microfluidic cytometry use planar detecting microelectrodes directly in contact with cell suspension to measure the electric signal or impedance changes. However, these methods not only require expensive electrodes printed on a circuit board, but also the microfabricated electrodes cannot be reused without a time-consuming cleaning process. We have overcome the shortcoming of the direct contact of the electrodes with the cell suspension in microfluidic cytometers by introducing the contactless conductivity measurement. The use of a contactless conductivity measurement offers the requirements of portability, universality and acceptable sensitivity. And they could avoid problems commonly found in the contact mode, including electrode fouling and bubble formation.

To the best of our knowledge, there are few published papers about microfluidic contactless impedance flow cytometry for single cell impedance^{3,31}. In a study on a microfluidic contactless impedance cytometer, a glass coverslip was used to separate the microfluidic channel and the sensing electrodes. The reusable planar electrodes were printed on a circuit board and impedance changes caused by the cells traversing the channel were measured contactlessly³. Nonetheless, impedance information as a function of the detection phase angle is not available with the C4D nor is it necessary when aiming only cell counting. Also that the C4D is advantageously simpler than an impedance analyzer because a fixed frequency is set and no phase locked loop detection circuitry is needed. When aiming only cell counting or sensing, C4D is much more necessary and preferable than an impedance analyzer. In addition, the ITO-coated glass, a price less than US\$1.00, is widely available in the market and opens up a new possibility of mass production of microfluidic chip-C4D devices in ordinary laboratories. In this paper, we focus on the microfluidic cytometer by integrating contactless conductivity sensor with the ITO detecting electrodes for cell sensing and counting.

We simulate the fluid flow in different designed microfluidic with Comsol software. As shown in Fig. S1A, the detecting microchannel is 10- μm -deep, while the transit microchannel is 60- μm -deep. When the detecting channel is 10- μm -deep, the fluid flow rate is much higher than the 20- μm -deep microchannel (Fig. S1B). As the HCM has a diameter of about 15 μm , we choose the 20- μm -deep microchannel which is a little larger than the tested cell size for cell sensing and cell counting analysis.

Based on the above simulation, the microchip is further investigated on the cell sensing and counting.

Theoretical analysis

Fig. 3A represents the circuit model of the microfluidic device. The three ITO electrodes and the microchannel together form the C4D detection system. The applied alternating current (AC) signal from the emitting electrode (the left ITO electrode) was coupled capacitively through the channel to the receiving electrode (the right ITO electrode). It can result in a small current that is amplified by an amplifier, rectified and offset-corrected using a rectifier, filtered by a low-pass filter. And it undergoes data acquisition using a data acquisition tool and finally recorded in a computer. In other words, the coupled signal of the same frequency was weaker at the receiving electrode with a negative phase shift. The current signal was subsequently amplified and converted into a voltage signal. The electrical signal by using a low-pass filter then biased to zero before it was sent to a data acquisition system for further measurement^{25,32}.

The C4D can be considered as a combination capacitor-resistor-capacitor electrical circuit. The electrodes and the channel's layer (glass) form the capacitors, and the section of the channel between the electrodes forms the resistor and capacitor. The background electrolyte solution can simply be modeled as a resistor. Its total impedance (Z) of the system (Fig. S2) can be expressed as:

$$Z = \frac{1}{j\omega C_y} + \frac{1}{1/r + j\omega C_x} = \frac{r}{1 + \omega^2 C_x^2 r^2} + j \frac{1 + \omega^2 C_x (C_x + C_y) r^2}{\omega C_y (1 + \omega^2 C_x^2 r^2)}$$

where r and C_x ($C_x=C_1$) are resistance and capacitance of the solution and cells in the

channel between two electrodes, respectively; C_y ($1/C_y = 1/C_2 + 1/C_3$) is the total capacitance between electrodes and solutions; ω is the angular frequency of the applied AC field.

In this case, the cell could be presented as a spherical and uniform conductive cytoplasm surrounded by a thin non-conductive membrane. When the tested cells are driven through the section of the microchannel between the detection electrodes, the measured impedance of the system changes instantaneously because of change in the resistance (r) and capacitance (C_x). When the capacitance of the cell (about 8.8×10^{-3} pF μm^{-1}) could be neglected, the resulting voltage signal varies linearly with the conductivity of the solution²³. So the change in the resistance is attributed to the different conductivity (conductivity = 1/resistivity) of different cell species passing through the detection electrodes with the background electrolyte solution. This leads to a sudden change in the level of the output voltage signal and appears as a peak in the data acquisition system, which can be measured by the computer. The analytical signal represents a variation of conductivity. Each peak is related by time to a specific cell, and the area under the peaks is related to the size of the specific cell. When cells of different sizes are flowing through the detection zone, the different electrical signals can be described in Fig. 3B. In the experiment, the electrical conductivities of the cancer cells and the background detection solution (in the microfluidic channel) are about 1×10^{-5} S m^{-1} and 1.7 S m^{-1} respectively^{3,15,33}. Based on the big difference of the conductivity value, the changes in the conductivity of solutions could result in a small change over the background signal for the microfluidic cytometer.

Figure 3

The distance between electrodes

Implementation of the standard detection gap for ITO electrodes turned out to be one of the most important steps of the experiments. It should be noted that the detection length determines the signal output and increasing the detection length by increasing the gap between the electrodes will reduce the output voltage³⁴. At the same time, it will also reduce the resolution or the ability to detect two different cells. Therefore, the distance between the emitting and receiving electrodes is of significance for the experiment. In this work, these microfluidic chips with various detection gaps from 1 mm to 3 mm were carried out. Experimental results showed that when the gap between the electrodes was set to 1 mm, the electrical signal was better than the others (data not shown). Meanwhile, Kuban and coworkers have demonstrated a standard distance of electrodes in C4D for microfluidic is usually 0.5-1 mm³⁵. Therefore, a gap distance of 1.0 mm was chosen for the following experimental study.

The baseline noise of different flow rates

Background noise has an important impact on the electrical signal detection. In general, different flow rates for C4D may contribute to the background signal and high flow rates result in high baseline noise. In this regard, a comparative experiment was performed. The performance of the C4D was examined for the five different flow rates and the effect on the background noise of the detector was employed. A 30 s portion of each electric record, which was depicted in Fig. 4A, showed that when flow

rates changed from 0 to 4 $\mu\text{L min}^{-1}$, the noise increased from 1.23 mV to 1.5 mV (Fig. 4B). Thus, no difference in stability was observed for the various flow rates, and that most of the rates used were suitable in that respect. Later experiments with cell suspension also indicated approximately electric signal for the two highest flow rates investigated. If we wanted to adjust the flow rate of the cells to make them move one by one into the detection channel, a slower flow rate was necessary. A flow rate of 2 $\mu\text{L min}^{-1}$ was therefore adopted for the microfluidic system.

Figure 4

Performance of the cytometer

In order to evaluate the accuracy of the designed microfluidic sensor, MCF-7 cells with different concentrations were measured using both the designed microfluidic cytometer device and a commercial cytometer. Four groups of cells were resuspended in PBS with specific concentrations (0, 5×10^3 , 1×10^4 , 3×10^4 cells mL^{-1}). A series of electrical signals for the detection of MCF-7 cells is shown in Fig. 5 A and B. Each peak indicates a tumor cell passes the detection area and the peak heights are depended on the cell volume or size. It is revealed that the size of the single cancer cell is different. The comparison of both results is shown in Fig. 5C, which shows a good accuracy between the developed microfluidic cytometer device and the commercial flow cytometer. This study demonstrates that the presented microfluidic cytometer is able to provide a reliable platform for cell sensing and counting, such as analysis of cancer cells. At a concentration of 5×10^3 cells mL^{-1} , this microfluidic cytometer exhibited a relative standard deviation (RSD) of 4% for

three determinations, indicating good repeatability.

Figure 5

To further evaluate the performance of the microfluidic cytometer, the electric signals of MCF-7 cells and HCM were determined by our approach separately. Fig. 6A shows the measured electrical signals for MCF-7 cells and HCM. It could be observed that a typical speed of $60 \text{ cells min}^{-1}$ in the cytometer was obtained and the cells can be detected separately when they were flowing through the detecting area. To detect cells with their different sizes, the height peaks which were caused by the cells passing through the microchannel can be measured. The fluorescence pictures of the MCF-7 and HCM cells provided that the cell surface area of HCM was much larger than the MCF-7 cells (Fig. S3). Since the MCF-7 cell is typically a sphere with a diameter of about $9 \mu\text{m}$, the HCM has a diameter of about $15 \mu\text{m}$. As shown in Fig. 6B, the signals of more than 70 % of MCF-7 cells were around 12 mV and the signals of more than 60 % of HCM were around 22 mV. Our data indicated that the discrimination of cells with different sizes can be achieved based on conductivity detection with our microfluidic cytometer.

Figure 6

All in all, the proposed microfluidic system revealed good results in detection of cells with acceptable accuracy and repeatability. This study has shown that the designed, cost-effective microfluidic cytometer built on ITO electrodes is capable of cell sensing and counting for point-of-care diagnosis. Although the throughput of the platform is lower than those of commercial cytometers, it could be used for sensing

and counting the small numbers of cells for home-use. Further studies can be focused on further improve the device throughput, reliability and sensitivity of the microfluidic sensing device, such as using a more sensitive data acquisition card, standardized fluorescent beads of different sizes and hydrodynamic sheath flow³⁶. From this perspective, there is still much effort needed to implement microfluidic sensors for commercial laboratories and real-world applications.

Conclusion

In conclusion, we have successfully designed, fabricated and demonstrated an integrated and cost-effective microfluidic contactless conductivity cytometer for cell sensing and counting. The platform contains a simple PDMS/glass microchip that can be inserted onto the ITO-coated glass with reusable ITO electrodes. The ITO electrode costs less than US\$1.00 and is widely available in the market. The glass plate is used as a barrier to isolate the electrodes from the buffer, allowing the electrodes to be easily reused. Furthermore, our experimental results have demonstrated that MCF-7 cells and HCM can be detected and counted with acceptable accuracy as compared to a commercial flow cytometer. This microfluidic cytometer can not only be applied for detecting and counting cells, but also be expected to become a promising tool for the label-free cell counting and point-of-care diagnosis, particularly in the resource-limited developing world.

Acknowledgements

This work was supported by the National Natural Science Foundation of China (Grant Nos. 21375152 and 21075139). The authors thank Prof. Peiqing Liu (New Drug

Screening Center, Sun Yat-Sen University) for the help in cell culture.

References

- 1 T. Hulgán, B. E. Shepherd, S. P. Raffanti, J. S. Fusco, R. Beckerman, G. Barkanic and T. R. Sterling, *J. Infect. Dis.*, 2007, **195**, 425-431.
- 2 D. Gao, H. F. Li, G. S. Guo and J. M. Lin, *Talanta*, 2010, **82**, 528-533.
- 3 S. Emaminejad, M. Javanmard, R. W. Dutton and R. W. Davis, *Lab Chip*, 2012, **12**, 4499-4507.
- 4 S. S. Khan, M. A. Solomon and J. P. McCoy, *Cytom. Part B-Clin. Cy.*, 2005, **64B**, 1-8.
- 5 J. Vives-Rego, P. Lebaron and G. Nebe-von Caron, *Fems. Microbiol. Rev.*, 2000, **24**, 429-448.
- 6 S. Joo, K. H. Kim, H. C. Kim and T. D. Chung, *Biosens. Bioelectron.*, 2010, **25**, 1509-1515.
- 7 Y. C. Chen, A. A. Nawaz, Y. H. Zhao, P. H. Huang, J. P. McCoy, S. J. Levine, L. Wang and T. J. Huang, *Lab Chip*, 2014, **14**, 916-923.
- 8 D. Erickson and D. Q. Li, *Anal. Chim. Acta*, 2004, **507**, 11-26.
- 9 Y. C. Tung, Y. S. Torisawa, N. Futai and S. Takayama, *Lab Chip*, 2007, **7**, 1497-1503.
- 10 Q. Q. Ji, G. S. Du, M. J. van Uden, Q. Fang and J. M. J. den Toonder, *Talanta*, 2013, **111**, 178-182.
- 11 H. J. Song, Y. Wang, J. M. Rosano, B. Prabhakarandian, C. Garson, K. Pant and E. Lai, *Lab Chip*, 2013, **13**, 2300-2310.
- 12 R. A. Erickson and R. Jimenez, *Lab Chip*, 2013, **13**, 2893-2901.

- 13 S. Gawad, L. Schild and P. Renaud, *Lab Chip*, 2001, **1**, 76-82.
- 14 H. G. Chun, T. D. Chung and H. C. Kim, *Anal. Chem.*, 2005, **77**, 2490-2495.
- 15 H. L. Gou, X. B. Zhang, N. Bao, J. J. Xu, X. H. Xia and H. Y. Chen, *J. Chromatogr. A*, 2011, **1218**, 5725-5729.
- 16 Y. Zheng, J. Nguyen, C. Wang and Y. Sun, *Lab Chip*, 2013, **13**, 3275-3283.
- 17 E. Du, S. Ha, M. Diez-Silva, M. Dao, S. Suresh and A. P. Chandrakasan, *Lab Chip*, 2013, **13**, 3903-3909.
- 18 J. H. Guo, H. G. Li, Y. Chen and Y. J. Kang, *Ieee Sens. J.*, 2014, **14**, 2112-2117.
- 19 J. Wang, G. Chen and A. Muck, *Talanta*, 2009, **78**, 207-211.
- 20 R. Nehme, H. Nehme, G. Roux, D. Cerniauskaite, P. Morin, P. Rollin and A. Tatibouet, *Anal. Chim. Acta*, 2014, **807**, 153-158.
- 21 P. Kuban and P. C. Hauser, *Electrophoresis*, 2015, **36**, 195-211.
- 22 R. M. Guijt, E. Baltussen, G. van der Steen, H. Frank, H. Billiet, T. Schalkhammer, F. Laugere, M. Vellekoop, A. Berthold, L. Sarro and G. W. K. van Dedem, *Electrophoresis*, 2001, **22**, 2537-2541.
- 23 W. K. T. Coltro, R. S. Lima, T. P. Segato, E. Carrilho, D. P. de Jesus, C. L. do Lago and J. A. F. da Silva, *Anal. Methods-UK*, 2012, **4**, 25-33.
- 24 P. Kuban and P. C. Hauser, *Electrophoresis*, 2011, **32**, 30-42.
- 25 Z. G. Chen, Q. W. Li, O. L. Li, X. Zhou, Y. Lan, Y. F. Wei and J. Y. Mo, *Talanta*, 2007, **71**, 1944-1950.
- 26 H. B. Qiu, J. L. Yan, X. H. Sun, J. F. Liu, W. D. Cao, X. R. Yang and E. K. Wang, *Anal. Chem.*, 2003, **75**, 5435-5440.

- 27 D. P. Sun, J. Lu, Z. G. Chen, Y. Y. Yu and Y. B. Li, *Microfluid. Nanofluid.*, 2014, **17**, 831-842.
- 28 B.Y. Xu, X.N. Yan, J.D. Zhang, J.J. Xu and H.Y. Chen, *Lab Chip*, 2012, **12**, 381-386.
- 29 N. Haandbaek, S. C. Burgel, F. Heer and A. Hierlemann, *Lab Chip*, 2014, **14**, 369-377.
- 30 Y. Zheng, E. Shojaei-Baghini, C. Wang and Y. Sun, *Biosens. Bioelectron.*, 2013, **42**, 496-502.
- 31 J. H. Guo, C. M. Li and Y. J. Kang, *Biomed. Microdevices*, 2014, **16**, 681-686.
- 32 J. Zhao, Z. G. Chen, X. C. Li and J. B. Pan, *Talanta*, 2011, **85**, 2614-2619.
- 33 C. G. Yao, X. Q. Hu, Y. Mi, C. X. Li and C. X. Sun, *Ieee T. Dielect. El. In.*, 2009, **16**, 1259-1266.
- 34 P. Kuban and P. C. Hauser, *Lab Chip*, 2005, **5**, 407-415.
- 35 P. Kuban and P. C. Hauser, *Lab Chip*, 2008, **8**, 1829-1836.
- 36 X. C. Xuan, J. J. Zhu and C. Church, *Microfluid. Nanofluid.*, 2010, **9**, 1-16.

Figure captions

Fig. 1 Schematic diagram (A) and photograph (B) of the designed microfluidic contactless conductivity cytometer.

Fig. 2 Structure and photograph of the microfluidic chip. (A) Schematic illustration for the three layered component and structure of the chip. (B) Photograph of the designed ITO-coated glass. (C) Photograph of the fabricated microfluidic chip. (D) Photograph of microfluidic detecting channel.

Fig. 3 Measurement schematic and principle of the C4D system. (A) Simplified equivalent circuit model of the C4D. r and C_1 : resistance and capacitance of the electrolyte solution and cells in the channel; C_2 or C_3 : capacitance between electrode and the solution; G is a amplifier converting current into voltage signals. (B) The schematics show that different cell sizes result in different electrical signals.

Fig. 4 Effect of the different flow rates on the noise of the C4D system. (A) The five different flow rates on the noise: (a) 0, (b) 0.5, (c) 1, (d) 2, (e) 4 $\mu\text{L min}^{-1}$. (B) Effect of the flow rate on the noise in the C4D. Conditions: excitation voltage 30 Vpp and frequency 60 kHz.

Fig.5 Electrical signals of the different concentration of MCF-7 cells: (A) 5×10^3 cells mL^{-1} and (B) 3×10^4 cells mL^{-1} . (C) Comparison of MCF-7 cell counting using the

designed microfluidic device and a commercial flow cytometer at different concentrations. Conditions: excitation voltage 30 Vpp and frequency 60 kHz.

Fig.6 Electrical signals and percentage distribution of MCF-7 and HCM cells. (A) Typical signals of MCF-7 and HCM cells measured by the microfluidic cytometer. (B) Histograms of the peak height distribution of MCF-7 cells (black bars) and HCM cells (red bars). Each histogram contains data from 180 cells for three experiments. Conditions: excitation voltage 30 Vpp and frequency 60 kHz.

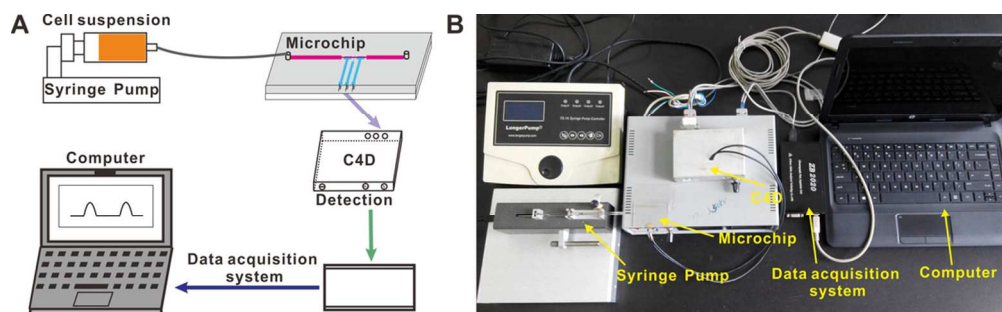


Fig. 1 Schematic diagram (A) and photograph (B) of the designed microfluidic contactless conductivity cytometer.
51x15mm (600 x 600 DPI)

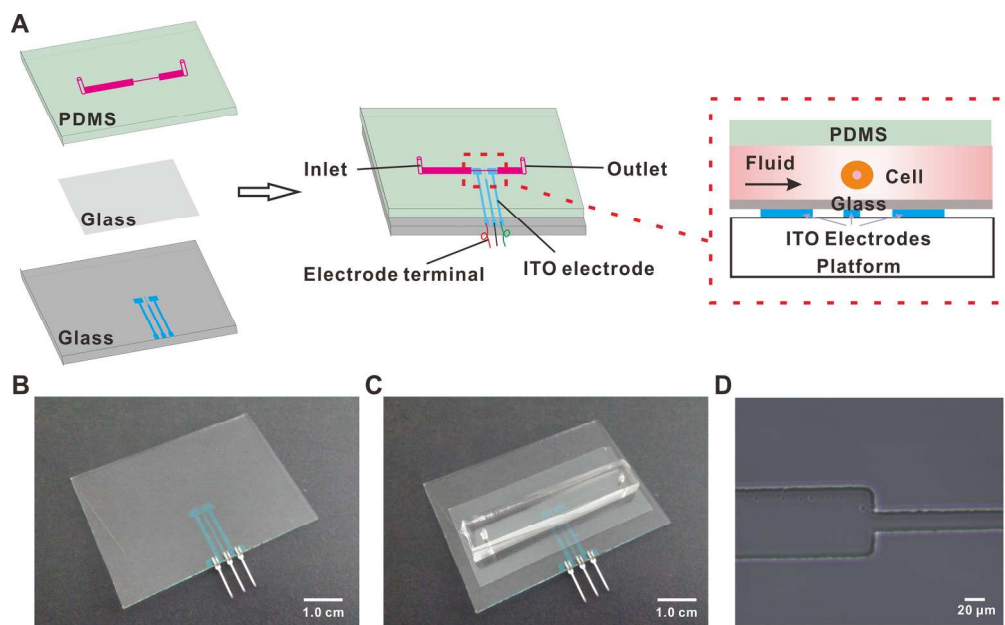


Fig. 2 Structure and photograph of the microfluidic chip. (A) Schematic illustration for the three layered component and structure of the chip. (B) Photograph of the designed ITO-coated glass. (C) Photograph of the fabricated microfluidic chip. (D) Photograph of microfluidic detecting channel. 97x59mm (600 x 600 DPI)

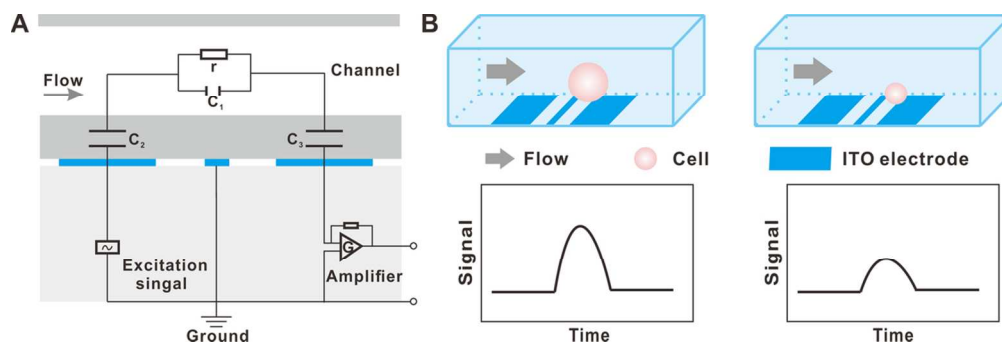


Fig. 3 Measurement schematic and principle of the C4D system. (A) Simplified equivalent circuit model of the C4D. r and C_1 : resistance and capacitance of the electrolyte solution and cells in the channel; C_2 or C_3 : capacitance between electrode and the solution; G is a amplifier converting current into voltage signals. (B) The schematics show that different cell sizes result in different electrical signals.
55x18mm (600 x 600 DPI)

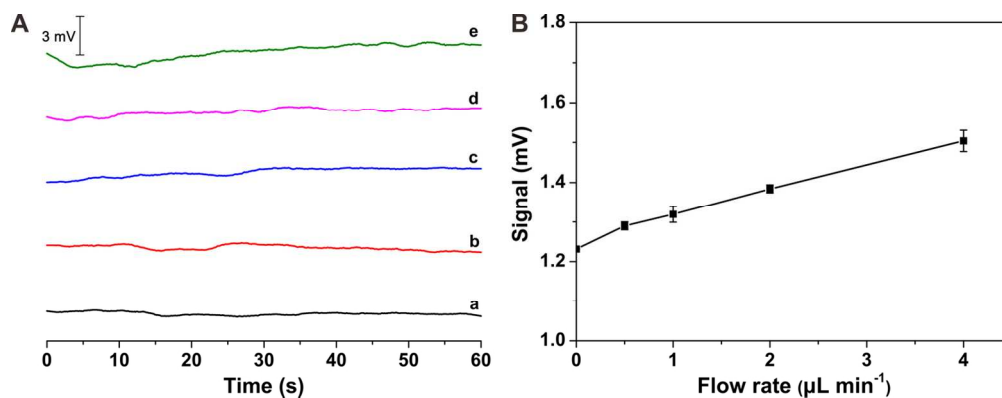


Fig. 4 Effect of the different flow rates on the noise of the C4D system. (A) The five different flow rates on the noise: (a) 0, (b) 0.5, (c) 1, (d) 2, (e) 4 $\mu\text{L min}^{-1}$. (B) Effect of the flow rate on the noise in the C4D. Conditions: excitation voltage 30 Vpp and frequency 60 kHz. 65x25mm (600 x 600 DPI)

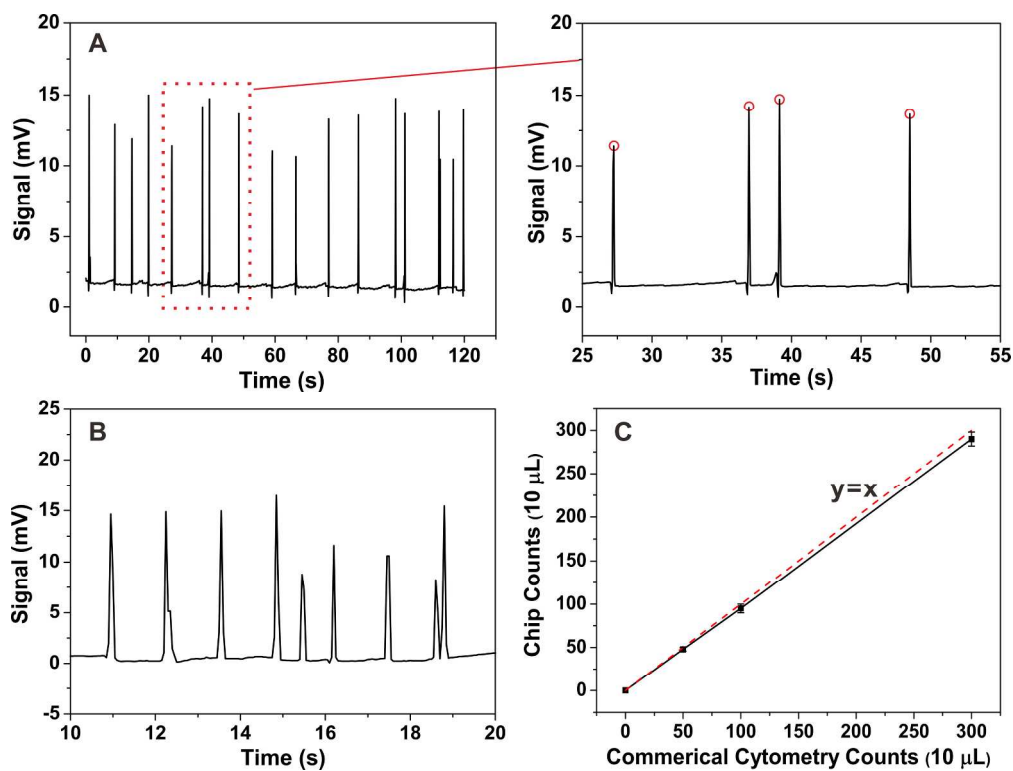


Fig.5 Electrical signals of the different concentration of MCF-7 cells: (A) 5×10^3 cells mL⁻¹ and (B) 3×10^4 cells mL⁻¹. (C) Comparison of MCF-7 cell counting using the designed microfluidic device and a commercial flow cytometer at different concentrations. Conditions: excitation voltage 30 Vpp and frequency 60 kHz. 120x91mm (600 x 600 DPI)

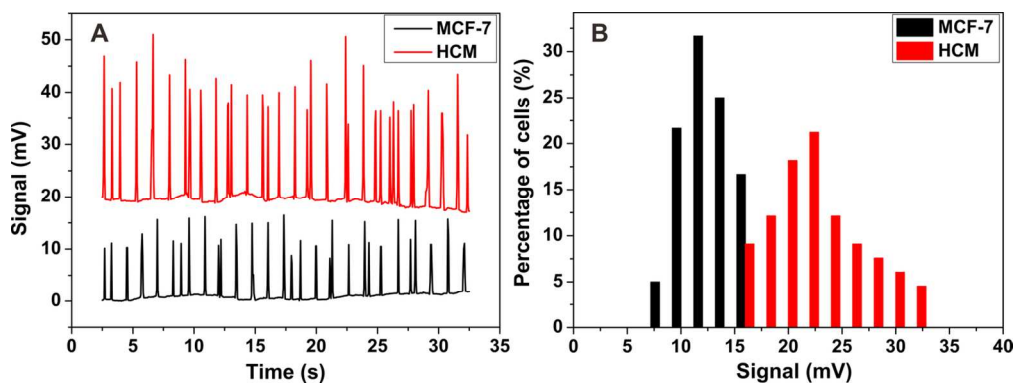


Fig.6 Electrical signals and percentage distribution of MCF-7 and HCM cells. (A) Typical signals of MCF-7 and HCM cells measured by the microfluidic cytometer. (B) Histograms of the peak height distribution of MCF-7 cells (black bars) and HCM cells (red bars). Each histogram contains data from 180 cells for three experiments. Conditions: excitation voltage 30 Vpp and frequency 60 kHz. 63x23mm (600 x 600 DPI)